Untangling the Electronic Band Structure of Wurtzite GaAs Nanowires by Resonant Raman Spectroscopy

Bernt Ketterer,[†] Martin Heiss,[†] Emanuele Uccelli,[†] Jordi Arbiol,[‡] and Anna Fontcuberta i Morral*[,†]

[†]Laboratoire des Matériaux Semiconducteurs, Institut des Matériaux, Ecole Polytechnique Fédérale de Lausanne, CH-1015 Lausanne, Switzerland and [‡]Institució Catalana de Recerca i Estudis Avançats (ICREA) and Institut de Ciència de Materials de Barcelona, ICMAB-CSIC, Campus de la UAB, E-08193 Bellaterra, CAT, Spain

ABSTRACT In semiconductor nanowires, the coexistence of wurtzite and zinc-blende phases enables the engineering of the electronic structure within a single material. This presupposes an exact knowledge of the band structure in the wurtzite phase. We demonstrate that resonant Raman scattering is a important tool to probe the electronic structure of novel materials. Exemplarily, we use this technique to elucidate the band structure of wurtzite GaAs at the Γ point. Within the experimental uncertainty we find that the free excitons at the edge of the wurtzite and the zinc-blende band gap exhibit equal energies. For the first time we show that the conduction band minimum in wurtzite GaAs is of Γ_7 symmetry, meaning a small effective mass. We further find evidence for a light-hole−heavy-hole splitting of 103 meV at 10 K.

KEYWORDS: electronic band structure · wurtzite GaAs · nanowires · resonant Raman

In recent years, semiconductor nanowires have attracted an enormous level of interest throughout the scientific community.[1−5] A particular feature of nanoscale materials is the formation of structural polytypes that are not stable in the bulk. This fascinating phenomenon has been observed in nanoparticles and nanowires.[6,7] Important semiconductors such as GaAs, GaP, InAs, InP, AlAs, AlP, GaSb, InSb, or Si are stable in the zinc-blende structure (ZB). They may crystallize in the wurtzite (WZ) lattice when they are grown in the nanowire form.[8−10] The change in the crystal symmetry from cubic to hexagonal implies a modification of the electronic band structure. The coexistence of WZ and ZB phases within a single nanowire opens unprecedented possibilities for band structure engineering and advanced nanowire devices.[11] For example, owing to the staggered band alignment between WZ and ZB GaAs, a quantum dot formed by an island of WZ (ZB) in a ZB (WZ) matrix would enable the longtime storage of holes (electrons). Alternatively, the formation of polytypic superlattices in silicon could eventually lead to the transformation in a direct bandgap material.[12,13] For the design of these novel structures, it is essential to have a clear picture of the band structure of the polytypes. Recently, materials scientists have achieved immense progress in controlling the crystal phase,[14−16] but only little experimental work has focused on the details of the electronic band structure of WZ arsenides, phosphides, and antimonides. Indeed, several groups reported microphotoluminescence measurements on the direct band gap of the WZ phase of InP,[17] InAs,[18] and GaAs. But in the presence of stacking faults, the interpretation of the spectra is often hindered by the simultaneous contribution of multiple confined WZ or ZB segments to the PL spectrum, and consequently the experimental results often diverged. For example, for the band gap of WZ GaAs values of 1.54,[19] 1.522,[20] 1.50,[21,22] and 1.519 eV[23] have been reported. The examination of the lower lying valence bands and higher conduction bands using photoluminescence techniques is even more challenging. Here, photoluminescence excitation spectroscopy could shed light on the valence band structure of InP,[24,25] and most recently, evidence for the second Γ_8 conduction band in heavily doped InP nanowires could be found in photoluminescence experiments.[26]

Resonant Raman spectroscopy (RRS) is a powerful tool in physical science that provides a vast plethora of information on the lattice dynamics, the electronic structure, the electron−phonon interaction, and the elementary excitations such as plasmons in both bulk and nanoscale materials. The key role of RRS in the interpretation of the unique vibrational spectrum of dimensionally confined carbon nanotubes,[27] or the recent progress in the understanding of quantum interference processes in the inelastic light scattering in graphene[28] are only two examples that illustrate this importance. In nanowires, the drastic consequences of a

* Address correspondence to anna.fontcuberta-morral@epfl.ch.

Received for review July 11, 2011 and accepted August 13, 2011.

Published online August 14, 2011
10.1021/nn202585j

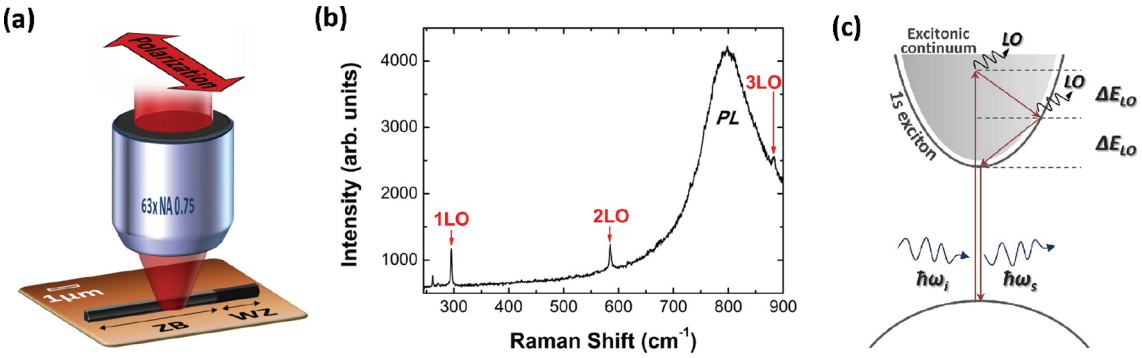

Figure 1. (a) Schematic drawing of the resonant micro-Raman experiment on a single nanowire. The linear polarized laser light is tuned over a wide energy range. (b) Near resonance multi-LO-phonon spectrum of an individual WZ GaAs nanowire. Scattering from up to three LO phonons is observed. The Raman spectrum is superimposed on a broad photoluminescence background. (c) Schematic diagram of the resonant Raman scattering from two LO phonons with the 1s exciton as the resonant intermediate state.

modified electron−phonon interaction on the optoelectronic properties has been demonstrated using the RRS technique.[29]

In the following, RRS is presented as an extremely suitable technique for the understanding of the electronic structure of nanoscale materials. The principle of this technique is shown in Figure 1a. The Raman scattering of a single nanostructure such as a nanowire is excited and collected locally with a spatial resolution of less than 1 μm. The microscopic picture of the Raman effect is usually described as the absorption and subsequent emission of a Raman scattered photon *via* a virtual intermediate electronic state. However, when the energy of the incident light approaches an interband transition of a semiconductor, real electronic states may mediate the thereby enhanced scattering process. As a consequence, direct information on the electronic band structure can be obtained by finding the conditions leading to resonant enhancement. In polar semiconductors the resonance is particularly important for the exciton-mediated scattering from longitudinal optical (LO) phonons. Here, not only the one-LO-phonon mode is strongly enhanced, but also the higher order multiphonon modes exhibit large enhancements.[30] An example of the multiphonon scattering from up to three LO in WZ GaAs nanowires is shown in Figure 1b. The resonant Raman scattering by two LO phonons can be described by the following sequence which is schematically shown in Figure 1c: (i) a photon is absorbed and a virtual exciton in a 1s state is created, (ii) the subsequent emission (or absorption) of two LO phonons causes the exciton to change its state, and (iii) the electronic system returns into the ground state by emission of a Raman scattered photon.[31] This process corresponds to the so-called "outgoing" resonance, where the strongest enhancement in the 2LO scattering is observed. Energy conservation within the global process requires that the energy of the incident photon exactly matches the energy of the band-edge exciton plus the energy of the two scattered LO phonons:

$$E_{\text{laser}} = E_{\text{exciton}} + E_{2\text{LO}} \quad (1)$$

By tuning the excitation energy, we can use the 2LO resonance profile to find the critical points of the band structure. Additionally, by measuring the polarization dependence of the resonance, information on the symmetry of the concerned bands can be obtained. Overall, RRS is an extremely suited technique for revealing the band structure of novel materials or structures, often synthesized in nanoscale sizes.

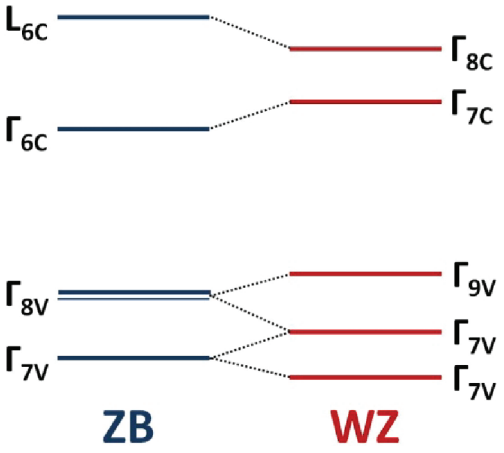

Figure 2. Schematic diagram showing the main differences in the band structure at the Γ and L point of a ZB semiconductor and the Γ point in the WZ phase. In the WZ phase, a conduction band with Γ_8 symmetry arises from the zonefolding of the L point in ZB to the Γ point in WZ.

A general comparison between the expected band structure of WZ and ZB semiconductors is shown in Figure 2. The differences in the band structure for WZ and ZB are multifold. First, the combination of both spin−orbit and crystal-field perturbations in WZ splits the cubic Γ_{15} valence states into the Γ_9 heavy-hole, Γ_7 light-hole, and Γ_7 crystal-field split-off valence bands in the hexagonal WZ structure. Furthermore, WZ exhibits a unit cell along the (0001) direction double as long as the one of ZB along the equivalent (111) direction. As a

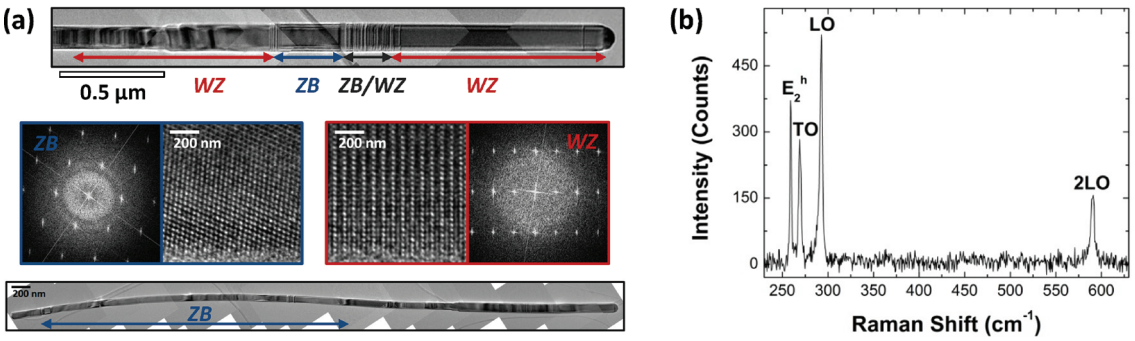

Figure 3. (a) HRTEM micrographs showing extended ZB GaAs parts at the base of the wire and long WZ segments at the nanowire tip. (b) Near-resonant micro-Raman spectrum from the WZ part of the nanowire exhibiting the characteristic E_2^h mode of the WZ structure.

consequence, there is a zone folding that leads to the existence of a supplementary conduction band in WZ with Γ_8 symmetry close to the ZB-like conduction band with Γ_7 symmetry. Interestingly, the Γ_8 band should exhibit a much larger electron mass than the Γ_7 conduction band.[32] In the case that WZ semiconductors would exhibit a Γ_8 conduction band minimum, one would expect the mobility of the material to be reduced significantly. This would have detrimental consequences for the transport properties and its device applicability. The symmetry of the lowest conduction band in WZ GaAs has been the subject of controversy in the past few years. Both Γ_8 and Γ_7 minima have been theoretically predicted.[32,33] Moreover, an experimental proof of the real nature of the conduction band minimum in WZ GaAs is, to the best of our knowledge, still missing. In a preliminary study we used RRS to examine the transition between the Γ_7 crystal-field split-off valence band and the Γ_7 conduction band in WZ GaAs. We found it lies at 1.982 eV at 0 K.[34] In this work, we extend our study in order to provide a clear picture of the band structure of WZ GaAs at the Γ point. We expect these results will be used in the future for further bandgap engineering using GaAs polytypes. Moreover, we expect that this work will open a new avenue for the investigation of the band structure of other novel materials and/or polytypes.

RESULTS AND DISCUSSION

A direct comparison of the band structure between WZ and ZB can be realized with a nanowire containing extended regions of the two phases. In a recent study, the direct correlation between the structure and optical properties of GaAs nanowires presenting a gradient in the WZ content enabled us to determine the value of the valence and conduction band discontinuities, as well as the bandgap deduced by the band-edge luminescence of 100% WZ nanowires.[21] Here, GaAs nanowires with large separated segments of ZB and WZ were investigated. The preferential growth of the WZ phase at the tip of the nanowire has been achieved by abrupt changes in the arsenic flux during the growth. The high resolution transmission electron microscopy (HRTEM) analysis of the nanowires is shown in Figure 3a. The first part of the nanowires presents long extensions of ZB structure with the presence of twins spaced for more than 1 μm. Interestingly, the abrupt change in the growth conditions also induces a cascaded increase in the nanowire diameter from 90 to 120 nm. This might be due to the increase in the Ga droplet size each time the V/III ratio is decreased. The tip of a nanowire is constituted by stacking fault-free segments of pure WZ GaAs with a length of greater than 1 μm. The WZ structure can be better appreciated and distinguished from the ZB in the detailed HRTEM micrograph insets in Figure 3a. A typical Raman spectrum of WZ GaAs taken near the resonance with the polarization of the incident light perpendicular to the hexagonal *c*-axis (parallel to the nanowire axis) is shown in Figure 3b. In all the Raman measurements from the WZ region, care was taken to ensure that the spectra were taken only at the nanowire tip to avoid any spurious effect related to the existence of stacking faults. In this scattering configuration, the Raman selection rules allow scattering from the E_1 transverse optical (TO) mode, as well as from the nonpolar E_2^h mode.[35] Resonant enhancement in the first-order scattering from LO phonons, as well as second-order scattering from two LO phonons is observed as well in the spectrum. The experiments were performed as follows. Raman spectra were collected as a function of the excitation energy between 1.72 and 1.57 eV for different incident polarizations. The intensity ratio between the LO or 2LO and the TO modes was then obtained as a function of the excitation conditions. Then, the resonant conditions were related to the critical points in the band structure. In the following, we present the enhancement of the LO and 2LO modes for the different configurations. The resonance profiles for first and second order scattering from LO phonons in the range of 1.67−1.72 eV are shown in Figure 4a. For both polarizations, parallel and perpendicular to the nanowire axis, we observe a strong outgoing resonance ($E_{laser} = E_{exciton} + E_{2LO}$) in the

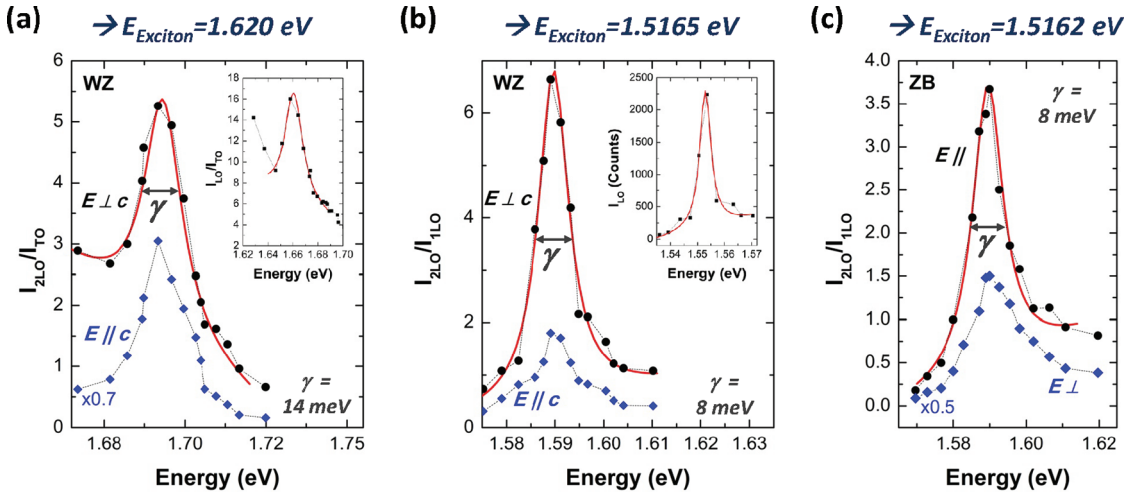

Figure 4. 2LO resonance profiles at the light-hole to Γ_7 conduction band transition in WZ GaAs (a) as well as at the bandgap of WZ GaAs (b) and ZB GaAs (c) for incident polarizations parallel and perpendicular to the nanowire axis. The insets in panels a and b show the one LO resonances at the corresponding WZ gaps. The profiles in panels a and c have been scaled for clarity. By displaying the 2LO/LO ratio, we remove the effect of the nanowire geometry in the coupling of the light into the nanowire for the two polarizations.

second order scattering from LO phonons with a maximum at 1.6932 eV and a width γ of 14 meV. The outgoing resonance in the first order scattering ($E_{laser} = E_{exciton} + E_{LO}$) occurs subsequently with an energy difference of one LO phonon. From the 2LO resonance condition $E_{laser} = E_{exciton} - E_{2LO}$ we calculate an energy $E_{exciton}$ of the observed free band-edge exciton in the WZ GaAs band structure of 1.620 eV at 10 K.

We now turn our attention to the band gap in WZ and ZB GaAs. The resonance profiles at the direct gap of WZ GaAs are shown in Figure 4b. From a Lorentzian fit we obtain the resonance maximum in the second order LO scattering at 1.5897 ± 0.0002 eV with a width of 8 meV. Subsequently, the resonance in the first order LO scattering occurs with the energy difference of one LO phonon. From eq 1 we obtain an energy of 1.5165 eV for the band-edge exciton at the fundamental bandgap in WZ GaAs. The 2LO resonance measured in a stacking fault-free ZB part of the GaAs nanowire is shown in Figure 4c. Interestingly, we obtain almost exactly the same energy as for the 2LO resonance in ZB GaAs. A Lorentzian fit results in a maximum at 1.5894 ± 0.0002 eV with a width of 8 meV for ZB GaAs, corresponding to a band-edge exciton energy of 1.5162 eV. It is an astonishing result that within the experimental uncertainty the numbers for WZ and ZB GaAs are equal. However, there is an important difference between the resonances observed in WZ and ZB GaAs. In Figure 4 panels b and c we see clearly that the 2LO resonance at the bandgap of WZ GaAs predominantly occurs for incident light polarized perpendicular to the hexagonal *c*-axis, whereas the 2LO resonance in ZB GaAs only weakly depends on the polarization of the incident laser light.

We continue with the discussion of the nature of the interband critical points based on the polarization dependence of the Raman resonances. Figure 5b demonstrates the weak dependence of the first 2LO resonance in WZ GaAs at $E_{exciton}$ = 1.620 eV on the incident polarization. We can understand this behavior from the optical selection rules for WZ crystals.[36,37] In Figure 5a the schematic of the band structure at the Γ point of a WZ crystal is shown together with the dipole allowed optical transitions for incident light polarized parallel or perpendicular to the hexagonal *c*-axis. For $E \perp c$, scattering from E_1 LO phonons allows coupling of states with symmetry $\Gamma_7 \rightarrow \Gamma_7$, $\Gamma_9 \rightarrow \Gamma_7$, and $\Gamma_9 \rightarrow \Gamma_8$, while for $E \parallel c$ the scattering from A_1 LO phonons allows only couples states with symmetry $\Gamma_7 \rightarrow \Gamma_7$.[38] Consequently, the unpolarized resonance at 1.620 eV can be unambiguously assigned with a transition from the Γ_7 light-hole valence band to the Γ_7 conduction band. The observed width of 14 meV, which is much greater than the corresponding width at the direct gap, is attributed to lifetime broadening due to the fast $\Gamma_7 \rightarrow \Gamma_9$ hole conversion by spontaneous phonon emission. As it can be seen in the measurement shown in Figure 5c, the resonance at the fundamental gap of ZB GaAs is unpolarized as expected for an optical transition from the degenerate Γ_8 valence band to the Γ_6 conduction band in crystals with ZB symmetry.[39] In contrast, the resonance at the fundamental gap in WZ GaAs is clearly polarized perpendicular to the hexagonal *c*-axis in Figure 5d. In this case, both the allowed $\Gamma_9 \rightarrow \Gamma_7$ and the $\Gamma_9 \rightarrow \Gamma_8$ transitions from the topmost heavy-hole valence band to the Γ_7 or Γ_8 conduction band have to be considered. In the following we will explain why only one of these two allowed transitions can be observed in the RRS experiment, and how we can identify the nature of the observed transition.

The most important question concerning the band structure of WZ GaAs is the symmetry of the lowest conduction band, as this will determine if the effective

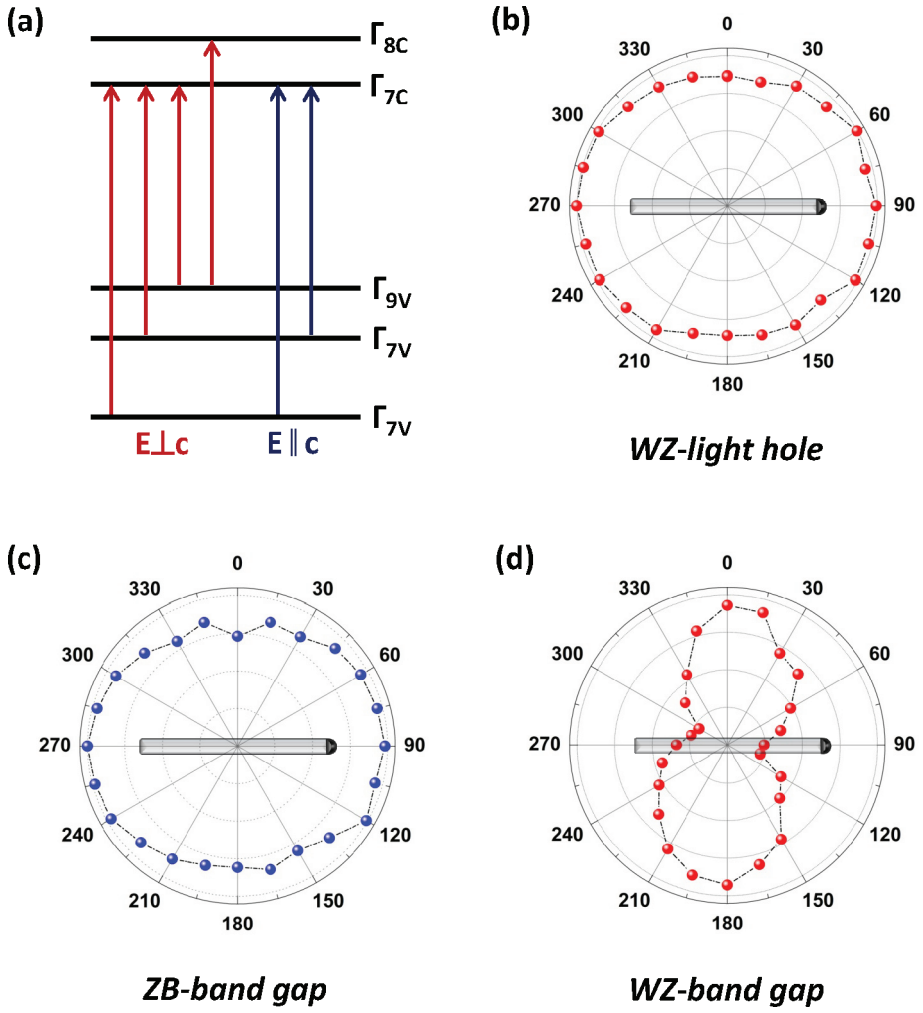

Figure 5. (a) Optical allowed transitions in a WZ crystal for incident polarization parallel and perpendicular to the hexagonal *c*-axis. (b–d) Dependence of the 2LO resonances on the incident polarization at the bandgap of WZ and ZB GaAs as well as at the light-hole to Γ_7 conduction band transition in WZ GaAs. The absolute 2LO intensities at the corresponding resonance maxima are plotted in the graphs. The orientation of the nanowire with respect to the polarization direction is shown schematically.

mass is extremely large or not. On the basis of symmetry considerations, it has been predicted that the lowest conduction band should have Γ_8 symmetry, provided that the band gap of the WZ phase is smaller than the ZB gap.[32,40] Our measurements are consistent with an equal or marginally higher bandgap. Now, two questions remain to be answered: (i) considering that both transitions from the topmost heavy-hole valence band to the Γ_7 or Γ_8 conduction bands are optically allowed, why do we observe a unique transition, and (ii) to what transition do the experiments correspond? Several arguments are consistent with the picture of a Γ_7 conduction band minimum. First of all, it should be difficult to observe a resonance with the Γ_8 band. It has been shown that in the WZ structure the optical matrix elements for zone center transitions between states that originate from the ZB Γ point and those arising from the back-folded ZB L-points should be rather small.[41,42] This is not the case for the transitions involving WZ Γ_7 states that originate from ZB zone center states, which is consistent with our observation of strong resonances for the transitions between the Γ_7 conduction band and the crystal-field split-off and the light-hole valence bands. A further argument that speaks for the Γ_7 nature of the conduction band minimum is the intensity of the 2LO scattering and the relation with the effective masses of electrons and holes. The effective mass of the electrons in the Γ_7 conduction band of WZ GaAs is much lower than the effective hole mass in the heavy-hole valence band. On the contrary, in the case of a heavy-hole band to Γ_8 conduction band transition the electron and hole effective masses are extremely similar.[32] It is known that for a similar mass between electrons and holes, the 2LO scattering efficiency decreases significantly.[31] Furthermore, the multiphonon resonant Raman spectra should exhibit a characteristic intensity alternation in which the even numbered LO lines are stronger than the odd-numbered lines, observed in InI and InBr.[43,44] On the contrary, in the case of polar semiconductors

with $m_e \ll m_h$ the intensity of the multi-LO-phonon scattered light decreases monotonically with increasing order,[45] in clear agreement with what we observe for WZ GaAs in Figure 1b. In views of all the arguments exposed here above, we assign the strong 2LO resonance at the band gap of WZ GaAs to the transition from the heavy-hole valence band to a conduction band minimum with low effective electron mass, which is the conduction band with Γ_7 symmetry. One should note here that while the value of the bandgap is in good agreement with the theoretical results from De and Pryor, the nature of the minimum conduction band is not.[32] Further studies are needed for understanding the nature of this discrepancy.

To summarize, we have obtained the following picture of the electronic band structure in WZ GaAs. As depicted in Figure 6, the energies of the free exciton at the heavy-hole ("A exciton"), light-hole ("B exciton"), and crystal-field split-off ("C exciton") valence band are found to be 1.517, 1.620, and 1.982 eV,[34] respectively. We find the lowest conduction band exhibits Γ_7 symmetry. Finally, it is possible to extract the spin−orbit splitting Δ_{so} and crystal-field-splitting Δ_{cr} using the quasicubic approximation:[46]

$$E_1 - E_{2,3} = \frac{1}{2}\left(\Delta_{cr} + \Delta_{so} \mp \sqrt{(\Delta_{cr}+\Delta_{so})^2 - \frac{8}{3}\Delta_{cr}\Delta_{so}}\right) \quad (2)$$

By applying eq 2 to our experimental results we obtain values of $\Delta_{so} = 0.379$ eV and $\Delta_{cr} = 0.189$ eV. The value of the spin−orbit splitting is in very good agreement with the predictions of De and Pryor ($\Delta_{so} = 0.351$ eV). However, the crystal field spitting is smaller than the value they predicted ($\Delta_{cr} = 0.244$ eV).[32] Meanwhile our experimental value for the crystal field splitting is larger than the value of $\Delta_{cr} = 0.122$ eV predicted in the pioneering theoretical work of Murayama and Nakayama.[33] The deviations might be because they assume an ideal WZ structure in their calculations. The experimental value could be altered due to quantum confinement effects or the presence of strain, though small for this type of nanowires.[35,47] In contrast, our value is in excellent agreement with most recent calculations

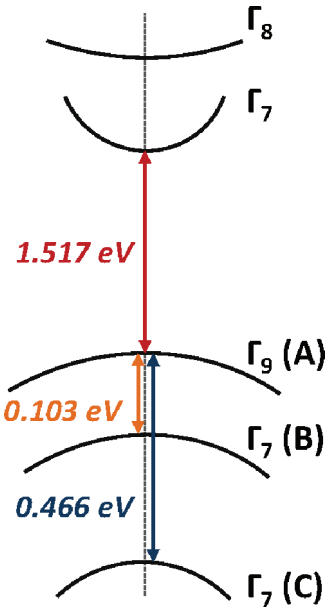

Figure 6. Band structure at the Γ point of WZ GaAs deduced from resonant Raman spectroscopy.

of Cheiwchanchamnangij and Lambrecht.[48] Within the GW approximation they obtained values of $\Delta_{cr} = 0.186$ eV using the LDA lattice constants and $\Delta_{cr} = 0.180$ eV using experimental data for the lattice volume.

CONCLUSION

We have shown that resonant Raman spectroscopy is a powerful tool to determine the electronic band structure in novel materials which may only exist on the nanoscale. By applying this technique to wurtzite GaAs nanowires, we measured the position of the three valence bands and the fundamental band gap. We find equal energies for the free exciton at the wurtzite and the zinc-blende band gap within our experimental error. Our experiments also indicate that the conduction band minimum in wurtzite GaAs is of Γ_7 symmetry. These results have strong implications for the future use of wurtzite GaAs nanowires for optoelectronic applications.

EXPERIMENTAL MATERIALS AND METHODS

Nanowire Growth. The nanowires were grown on the native oxide of an undoped Si (111) wafer in a gallium-assisted process by molecular beam epitaxy using a DCA P600 MBE machine.[49−51] To obtain the sequence of ZB and WZ, we varied the As_4 flux during growth.[21,52] We first started the growth for 1 h under our standard conditions that lead to stacking-fault free ZB GaAs nanowires, that is to say a gallium partial pressure of 6.17×10^{-8} Torr, an arsenic partial pressure of 2×10^{-6} Torr, and a temperature of 630 °C. Then, we consecutively decreased the V/III ratio from 32.4 to 6.9. for 1, 5, and 30 min. In between, the growth was continued each time for 30 min at the initial V/III ratio. As a result, we obtained a preferential growth of WZ GaAs at the tip of the nanowires.[52]

Characterization. Raman scattering experiments were performed in backscattering geometry on single nanowires at 10 K using a tunable titanium−sapphire laser as excitation source. The light was focused on the sample by a diffraction limited spot of <1 μm with an objective of N.A. = 0.75. A triple spectrometer was used in order to separate the weak Raman scattered light from the intense Rayleigh scattered light. The signal was collected in a multichannel charged-coupled device.

Acknowledgment. The authors acknowledge financial support from the Swiss National Science Foundation through Grant No. 2000021-121758/1 and No. 129775/1, the NCCR on "Quantum Science and Technology", and the European Research Council under the UpCon grant. J.A. acknowledges the funding from the Spanish MICINN (MAT2010-15138 (COPEON)) and Generalitat de Catalunya (2009 SGR 770 and XaRMAE).

REFERENCES AND NOTES

1. Cui, Y.; Lieber, C. M. Functional Nanoscale Electronic Devices Assembled Using Silicon Nanowire Building Blocks. *Science* **2001**, *291*, 851–853.
2. Gudiksen, M. S.; Lauhon, L. J.; Wang, J.; Smith, D. C.; Lieber, C. M. Growth of Nanowire Superlattice Structures for Nanoscale Photonics and Electronics. *Nature* **2002**, *415*, 617–620.
3. Johansson, J.; Karlsson, L. S.; Svensson, C. P. T.; Mårtensson, T.; Wacaser, B. A.; Deppert, K.; Samuelson, L.; Seifert, W. Structural Properties of (111)B-Oriented III–V Nanowires. *Nat. Mater.* **2006**, *5*, 574–580.
4. Qian, F.; Gradečak, S.; Li, Y.; Park, H.-G.; Dong, Y.; Ding, Y.; Wang, Z. L.; Lieber, C. M. Multiquantum-Well Nanowire Heterostructures for Wavelength-Controlled Lasers. *Nat. Mater.* **2008**, *7*, 701–706.
5. Nadj-Perge, S.; Frolov, S. M.; Bakkers, E. P. A. M.; Kouwenhoven, L. P. Spin-Orbit Qubit in a Semiconductor Nanowire. *Nature* **2010**, *468*, 1084–1087.
6. Chen, C.-C.; Herhold, A. B.; Johnson, C. S.; Alivisatos, A. P. Size Dependence of Structural Metastability in Semiconductor Nanocrystals. *Science* **1997**, *276*, 398–401.
7. Viera, G.; Mikikian, M.; Bertran, E.; i Cabarrocas, P. R.; Boufendi, L. Atomic Structure of the Nanocrystalline Si Particles Appearing in Nanostructured Si Thin Films Produced in Low-Temperature Radiofrequency Plasmas. *J. Appl. Phys.* **2002**, *92*, 4684–4694.
8. Lopez, F. J.; Hemesath, E. R.; Lauhon, L. J. Ordered Stacking Fault Arrays in Silicon Nanowires. *Nano Lett.* **2009**, *9*, 2774–2779.
9. Fontcuberta i Morral, A.; Arbiol, J.; Prades, J. D.; Cirera, A.; Morante, J. R. Synthesis of Silicon Nanowires with Wurtzite Crystalline Structure by Using Standard Chemical Vapor Deposition. *Adv. Mater.* **2007**, *19*, 1347–1351.
10. Kriegner, D.; Panse, C.; Mandl, B.; Dick, K. A.; Keplinger, M.; Persson, J. M.; Caroff, P.; Ercolani, D.; Sorba, L.; Bechstedt, F.; *et al.* Unit Cell Structure of Crystal Polytypes in InAs and InSb Nanowires. *Nano Lett.* **2011**, *11*, 1483–1489.
11. Caroff, P.; Bolinsson, J.; Johansson, J. Crystal Phases in III–V Nanowires: From Random Toward Engineered Polytypism. *IEEE J. Sel. Top. Quant. Electron* **2011**, *17*, 829–846.
12. Akopian, N.; Patriarche, G.; Liu, L.; Harmand, J.-C.; Zwiller, V. Crystal Phase Quantum Dots. *Nano Lett.* **2010**, *10*, 1198–1201.
13. Ikonic, Z.; Srivastava, G. P.; Inkson, J. C. Optical Properties of Twinning Superlattices in Diamond-Type and Zinc-Blende-Type Semiconductors. *Phys. Rev. B* **1995**, *52*, 14078–14085.
14. Algra, R. E.; Verheijen, M. A.; Borgstrom, M. T.; Feiner, L.-F.; Immink, G.; van Enckevort, W. J. P.; Vlieg, E.; Bakkers, E. P. A. M. Twinning Superlattices in Indium Phosphide Nanowires. *Nature* **2008**, *456*, 369–372.
15. Dick, K. A.; Thelander, C.; Samuelson, L.; Caroff, P. Crystal Phase Engineering in Single InAs Nanowires. *Nano Lett.* **2010**, *10*, 3494–3499.
16. Bolinsson, J.; Caroff, P.; Mandl, B.; Dick, K. A. Wurtzite–Zincblende Superlattices in InAs Nanowires Using a Supply Interruption Method. *Nanotechnology* **2011**, *22*, 265606.
17. Mishra, A.; Titova, L. V.; Hoang, T. B.; Jackson, H. E.; Smith, L. M.; Yarrison-Rice, J. M.; Kim, Y.; Joyce, H. J.; Gao, Q.; Tan, H. H.; *et al.* Polarization and Temperature Dependence of Photoluminescence from Zincblende and Wurtzite InP Nanowires. *Appl. Phys. Lett.* **2007**, *91*, 263104.
18. Sun, M. H.; Leong, E. S. P.; Chin, A. H.; Ning, C. Z.; Cirlin, G. E.; Samsonenko, Y. B.; Dubrovskii, V. G.; Chuang, L.; Chang-Hasnain, C. Photoluminescence Properties of InAs Nanowires Grown on GaAs and Si Substrates. *Nanotechnology* **2010**, *21*, 335705.
19. Hoang, T. B.; Moses, A. F.; Zhou, H. L.; Dheeraj, L.; Fimland, O.; Weman, H. Observation of Free Exciton Photoluminescence Emission from Single Wurtzite GaAs Nanowires. *Appl. Phys. Lett.* **2009**, *94*, 133105.
20. Martelli, F.; Piccin, M.; Bais, G.; Jabeen, F.; Ambrosini, S.; Rubini, S.; Franciosi, A. Photoluminescence of Mn-Catalyzed GaAs Nanowires Grown by Molecular Beam Epitaxy. *Nanotechnology* **2007**, *18*, 125603.
21. Heiss, M.; Conesa-Boj, S.; Ren, J.; Tseng, H.-H.; Gali, A.; Rudolph, A.; Uccelli, E.; Peiró, F.; Morante, J. R.; Schuh, D.; *et al.* Direct Correlation of Crystal Structure and Optical Properties in Wurtzite/Zinc-Blende GaAs Nanowire Heterostructures. *Phys. Rev. B* **2011**, *83*, 045303.
22. Moewe, M.; Chuang, L. C.; Crankshaw, S.; Chase, C.; Chang-Hasnain, C. Atomically Sharp Catalyst-Free Wurtzite GaAs-AlGaAs Nanoneedles Grown on Silicon. *Appl. Phys. Lett.* **2008**, *93*, 023116.
23. Chuang, L. C.; Moewe, M.; Ng, K. W.; Tran, T.-T. D.; Crankshaw, S.; Chen, R.; Ko, W. S.; Chang-Hasnain, C. GaAs Nanoneedles Grown on Sapphire. *Appl. Phys. Lett.* **2011**, *98*, 123101.
24. Perera, S.; Pemasiri, K.; Fickenscher, M. A.; Jackson, H. E.; Smith, L. M.; Yarrison-Rice, J.; Paiman, S.; Gao, Q.; Tan, H. H.; Jagadish, C. Probing Valence Band Structure in Wurtzite InP Nanowires Using Excitation Spectroscopy. *Appl. Phys. Lett.* **2010**, *97*, 023106.
25. Gadret, E. G.; Dias, G. O.; Dacal, L. C. O.; de Lima, M. M.; Ruffo, C. V. R. S.; Iikawa, F.; Brasil, M. J. S. P.; Chiaramonte, T.; Cotta, M. A.; Tizei, L. H. G.; *et al.* Valence-Band Splitting Energies in Wurtzite InP Nanowires: Photoluminescence Spectroscopy and *ab Initio* Calculations. *Phys. Rev. B* **2010**, *82*, 125327.
26. Wallentin, J.; Mergenthaler, K.; Ek, M.; Wallenberg, L. R.; Samuelson, L.; Deppert, K.; Pistol, M.-E.; Borgström, M. T. Probing the Wurtzite Conduction Band Structure Using State Filling in Highly Doped InP Nanowires. *Nano Lett.* **2011**, *11*, 2286–2290.
27. Rao, A. M.; Richter, E.; Bandow, S.; Chase, B.; Eklund, P. C.; Williams, K. A.; Fang, S.; Subbaswamy, K. R.; Menon, M.; Thess, A.; *et al.* Diameter-Selective Raman Scattering from Vibrational Modes in Carbon Nanotubes. *Science* **1997**, *275*, 187–191.
28. Chen, C. F.; Park, C.-H.; Boudouris, B. W.; Horng, J.; Geng, B.; Girit, C.; Zettl, A.; Crommie, M. F.; Segalman, R. A.; Louie, S. G.; *et al.* Controlling Inelastic Light Scattering Quantum Pathways in Graphene. *Nature* **2011**, *471*, 617–620.
29. Brewster, M.; Schimek, O.; Reich, S.; Gradečak, S. Exciton-Phonon Coupling in Individual GaAs Nanowires Studied Using Resonant Raman Spectroscopy. *Phys. Rev. B* **2009**, *80*, 201314.
30. Yu, P. Y.; Cardona, M. *Fundamentals of Semiconductors*; Springer: Berlin/Heidelberg, 2010.
31. Garca-Cristóbal, A.; Cantarero, A.; Trallero-Giner, C.; Cardona, M. Excitonic Model for Second-Order Resonant Raman Scattering. *Phys. Rev. B* **1994**, *49*, 13430–13445.
32. De, A.; Pryor, C. E. Predicted Band Structures of III–V Semiconductors in the Wurtzite Phase. *Phys. Rev. B* **2010**, *81*, 155210.
33. Murayama, M.; Nakayama, T. Chemical Trend of Band Offsets at Wurtzite/Zinc-Blende Heterocrystalline Semiconductor Interfaces. *Phys. Rev. B* **1994**, *49*, 4710–4724.
34. Ketterer, B.; Heiss, M.; Livrozet, M. J.; Rudolph, A.; Reiger, E.; Fontcuberta i Morral, A. Determination of the Band Gap and the Split-Off Band in Wurtzite GaAs Using Raman and Photoluminescence Excitation Spectroscopy. *Phys. Rev. B* **2011**, *83*, 125307.
35. Zardo, I.; Conesa-Boj, S.; Peiro, F.; Morante, J. R.; Arbiol, J.; Uccelli, E.; Abstreiter, G.; Fontcuberta i Morral, A. Raman Spectroscopy of Wurtzite and Zinc-Blende GaAs Nanowires: Polarization Dependence, Selection Rules, and Strain Effects. *Phys. Rev. B* **2009**, *80*, 245324.
36. Tronc, P.; Kitaev, Y.; Wang, G.; Limonov, M.; Panfilov, A.; Neu, G. Optical Selection Rules for Hexagonal GaN. *Phys. Status Solidi B* **1999**, *216*, 599–603.

37. Thomas, D. G.; Hopfield, J. J. Optical Properties of Bound Exciton Complexes in Cadmium Sulfide. *Phys. Rev.* **1962**, *128*, 2135–2148.
38. Richter, W. *Solid-State Physics*; Springer Tracts in Modern Physics, Vol 78; Springer: Berlin/Heidelberg, 1976; pp 121−272.
39. Birman, J. L. Polarization of Fluorescence in CdS and ZnS Single Crystals. *Phys. Rev. Lett.* **1959**, *2*, 157–159.
40. Yeh, C.-Y.; Wei, S.-H.; Zunger, A. Relationships Between the Band Gaps of the Zinc-Blende and Wurtzite Modifications of Semiconductors. *Phys. Rev. B* **1994**, *50*, 2715–2718.
41. Cardona, M.; Harbeke, G. Optical Properties and Band Structure of Wurtzite-Type Crystals and Rutile. *Phys. Rev.* **1965**, *137*, A1467–A1476.
42. Cardona, M. Band Parameters of Semiconductors with Zincblende, Wurtzite, and Germanium Structure. *J. Phys. Chem. Solids* **1963**, *24*, 1543–1555.
43. Ohno, N.; Yoshida, M.; Nakamura, K.; Nakai, Y. Multiple LO Scattering in Indium Iodide. *Solid State Commun.* **1985**, *53*, 569–572.
44. Mitsutake, H.; Yoshida, M.; Nakamura, K.; Nakai, Y. Resonant Light Scattering in InBr: Intensity Alternation of Multiple LO Phonon Scattering. *J. Phys. Soc. Jpn.* **1986**, *55*, 1070–1073.
45. Trallero-Giner, C.; Riera, R. Multiple LO-Phonon Raman Scattering and Hot Excitons. *Phys. Status Solidi B* **1989**, *152*, 357–367.
46. Chuang, S. L.; Chang, C. S. KP Method for Strained Wurtzite Semiconductors. *Phys. Rev. B* **1996**, *54*, 2491–2504.
47. Spirkoska Jovanov, D. *Fundamental Properties of Self-Catalyzed GaAs Nanowires and Related Heterostructures*; Selected Topics of Semiconductor Physics and Technology, Vol. 120; Verein zur Förderung des Walter Schottky Instituts der Technischen Universität München: Germany, 2010;
48. Cheiwchanchamnangij, T.; Lambrecht, W. R. L. Band Structure Parameters of Wurtzite and Zinc-Blende GaAs under Strain in the GW Approximation. *Phys. Rev. B* **2011**, *84*, 035203.
49. Colombo, C.; Spirkoska, D.; Frimmer, M.; Abstreiter, G.; Fontcuberta i Morral, A. Ga-Assisted Catalyst-Free Growth Mechanism of GaAs Nanowires by Molecular Beam Epitaxy. *Phys. Rev. B* **2008**, *77*, 155326.
50. Spirkoska, D.; Colombo, C.; Heiss, M.; Abstreiter, G.; i Morral, A. F. The Use of Molecular Beam Epitaxy for the Synthesis of High Purity III−V Nanowires. *J. Phys. Cond. Matter* **2008**, *20*, 454225.
51. Uccelli, E.; Arbiol, J.; Magen, C.; Krogstrup, P.; Russo-Averchi, E.; Heiss, M.; Morier-Genoud, F.; Morante, J. R.; Nygård, J.; Fontcuberta i Morral, A. Three-Dimensional Twinning of Self-Catalyzed GaAs Nanowires on Si Substrates. *Nano Lett.*, published online August 8, 2011; DOI: 10.1021/nl201902w.
52. Spirkoska, D.; Arbiol, J.; Gustafsson, A.; Conesa-Boj, S.; Glas, F.; Zardo, I.; Heigoldt, M.; Gass, M. H.; Bleloch, A. L.; Estrade, S.; *et al.* Structural and Optical Properties of High Quality Zinc-Blende/Wurtzite GaAs Nanowire Heterostructures. *Phys. Rev. B* **2009**, *80*, 245325.